FIRE AND MATERIALS
*Fire Mater.* (2009)
Published online in Wiley InterScience (www.interscience.wiley.com). DOI: 10.1002/fam.1024

# Fire effluent component yields from room-scale fire tests[‡,§]

Richard G. Gann[*,†], Jason D. Averill, Erik L. Johnsson, Marc R. Nyden and Richard D. Peacock

*Fire Research Division, Building and Fire Research Laboratory, National Institute of Standards and Technology, Gaithersburg, MD 20899-8664, U.S.A.*

SUMMARY

Estimation of the time available for escape (ASET) in the event of a fire is a principal component in fire hazard or risk assessment. Valid data on the yields of toxic smoke components from bench-scale apparatus is essential to accurate ASET calculations. This paper presents a methodology for obtaining pre-flashover and post-flashover toxicant yields from room-scale fire tests. The data are to be used for comparison with bench-scale data for the same combustibles: a sofa, bookcases, and electric power cable. Each was burned in a room with a long adjacent corridor. The yields of $CO_2$, CO, HCl, HCN, and soot were determined. Other toxicants ($NO_2$, formaldehyde, and acrolein), whose concentrations were below the detection limits, were of limited importance relative to the detected toxicants. The uncertainty values were comparable to those estimated for calculations used to determine ASET and were sufficiently small to determine whether a bench-scale apparatus is producing results that are similar to the real-scale results here. The use of Fourier transform infrared spectroscopy was useful for obtaining toxicant concentration data; however, its operation and interpretation are not routine. The losses of CO, HCN, and HCl along the corridor were dependent on the combustible. Copyright © 2009 John Wiley & Sons, Ltd.

Received 11 August 2009; Revised 6 November 2009; Accepted 10 November 2009

KEY WORDS: fire; fire research; smoke; room fire tests; fire toxicity; smoke toxicity; toxicity

*Correspondence to: Richard G. Gann, Fire Research Division, Building and Fire Research Laboratory, National Institute of Standards and Technology, Gaithersburg, MD 20899-8664, U.S.A.
†E-mail: rggann@nist.gov

‡This paper is a product of the National Institute of Standards and Technology and is not subject to copyright in the United States.

§Certain commercial entities, equipment, or materials may be identified in this document in order to describe an experimental procedure or concept adequately. Such identification is not intended to imply recommendation or endorsement by the National Institute of Standards and Technology, nor is it intended to imply that the entities, materials, or equipment are necessarily the best available for the purpose.

Contract/grant sponsors: National Institute of Standards and Technology, the Alliance for the Polyurethane Industry, the American Plastics Council, DuPont, Lamson & Sessions, Underwriters Laboratories, and the Vinyl Institute under the aegis of the Fire Protection Research Foundation

## 1. INTRODUCTION

Estimation of the time people will have available to escape (ASET) or find a place of refuge in the event of a fire is a principal component of the fire hazard or risk assessment of an occupancy. Accurate assessment enables public officials and facility owners to provide a selected or mandated degree of fire safety with both flexibility of design and confidence in the outcome. Inaccurate assessment can result in a degree of safety other than that desired and increased cost and/or rejection of otherwise desirable building and furnishing products.

The computation in such an assessment involves the building design, the capabilities of the occupants, the potential growth rate of a fire, the spread rate of the heat and smoke, and the impact of the fire effluent (toxic gases, aerosols, and heat) on people in the fire vicinity, both occupants and responders [1]. Simulating the fire and the resulting dispersal of fire effluent can be effected using a computational fluid dynamics (CFD) model, such as the fire dynamics simulator (FDS) [2], or a zone model, such as CFAST [3]. Such models can provide detailed information about the time-dependent concentrations of toxic gases throughout the building, provided that information exists about the yields of toxic gases from the materials involved in the fire. Times to untenability can be calculated from these concentrations using the equations in ISO 13571 [4], which comprise a consensus among international experts in fire toxicology and fire science of the best available information on incapacitation of people by exposure to toxic gases, heat, and smoke.[¶]

Combined, these components enable the estimation of ASET. A key remaining component is the identification of reliable means for obtaining the needed input data regarding the output of the fire.

Historically, such data were obtained in the form of an $EC_{50}$, the concentration of combustion effluent that caused a particular effect on laboratory animals (almost always rodents), either within a fixed exposure time or within that time plus a fixed post-exposure period. Lethality was the effect most frequently measured, with some measurements having been made of incapacitation [5]. Analysis of these data indicated that the lethal exposure was approximately double the incapacitating exposure [5, 6]. A number of bench-scale[‖] methods have been used to obtain such numbers [7].

There are, however, limitations to the use of animals for such a purpose. First, while they do integrate the effects of the potentially hundreds of combustion products, the effect on the rodents needs to be extrapolated to people. Second, there are relatively few laboratories that perform such animal-based assays. Third, there is reluctance in some jurisdictions to require routine animal testing.

As a result, attention has shifted to the measurement of the chemical yields of known toxic combustion products. As mentioned above, some technology exists for calculating the transport of these species and for estimating their impact on people. However, in the absence of an animal test, there is no way to determine whether one or more important toxicants were not measured or were even unidentified.

Fortunately, the general experience has been that the lethal toxic potency of fire effluent can very frequently be reasonably characterized by a small number, $N$, of toxic gases. This N-gas set forms the basis for the equations in ISO 13571 (See below.)

[¶] Incapacitation is defined as the inability of a person to effect one's own escape or to find a place of safe refuge.

[‖] These 'bench-scale' apparatus are characterized by their use of a relatively small test specimen, cut from the finished product of interest, and a combustor designed to approximate the thermal environment to which the finished product would be exposed in an actual fire.



DOI: 10.1002/fam

ISO TC92 SC3, Fire Threat to People and the Environment, has generated guidelines for assessing the fire threat to people [8] and addressed the issue of identifying bench-scale devices that can provide accurate input data for fire hazard and risk assessment. ISO 16312-1 provides general guidance and specific criteria [9]. ISO/TR 16312-2 appraises 12 bench-scale apparatus against these criteria [10].

The National Institute of Standards and Technology (NIST) is conducting research to establish quantitative measures of accuracy for such bench-scale methods. This paper comprises the first step in this process. We report here the results of room-scale fire tests in which four combustibles were burned in an unconfined room–corridor facility. Both pre-flashover and post-flashover measurements were made of the concentrations of toxicants, $O_2$, and smoke particulate in the upper layer of the burn room and at two locations in the upper layer of an external, open-ended corridor. In two tests with the room doorway blocked, the effluent was sampled from the upper layer of the burn room. Yields of the toxic gases were calculated using the consumed mass of the fuel, the measured gas concentrations, and data regarding the flow down the corridor. Since some of the toxicants might be removed from the inhalable environment during flow down the corridor, the corridor data were used to estimate a degree of loss of each toxicant. Where a concentration was too low to be measured, an upper limit was estimated. A complementary report contains additional details of this work [11].

Continuing research involves combusting the same fuels in typical bench-scale apparatuses under combustion conditions appropriate to well-ventilated and ventilation-limited burning. The information generated in these real-scale fire tests then comprises the basis for assessing the accuracy of the yields from the various bench-scale devices.

## 2. EXPERIMENTAL INFORMATION

### *2.1. Fire test configuration*

The tests were conducted in the two-compartment assembly shown schematically in Figure 1 and photographically in Figure 2. The interior of the burn room was 2.44 m wide, 2.44 m high, and 3.66 m long. The attached corridor was 9.75 m long and of the same width and height as the burn room. A doorway 0.76 m wide and 2.0 m high was centered in the common wall. The downstream end of the corridor was fully open, i.e. there was no end wall. A vent in the corridor ceiling enabled measurement of heat release rate; this vent was closed during nearly all the tests reported here. The entire assembly was elevated 0.76 m on cinder block supports. Sheets of calcium silicate board lined the surfaces of the walls and ceilings of the burn room and the upstream 2.44 m portion of the corridor. The downstream portion of the corridor was lined with gypsum wall board.

### *2.2. Instrumentation*

*Mass.* Either of two load cells was used to measure the specimen mass loss during the tests. The load cells were placed on the floor of the test bay below the burn room. The combustible was placed on a large metal pan that was in turn supported on a frame that transmitted the mass through holes in the burn room floor to the load cell. The load cell for the primary combustibles (see below) had a capacity of 1000 kg with a rated resolution of 0.5 kg. The load cell for the PVC sheet had a capacity of 150 kg with a rated resolution of 2 g.



DOI: 10.1002/fam

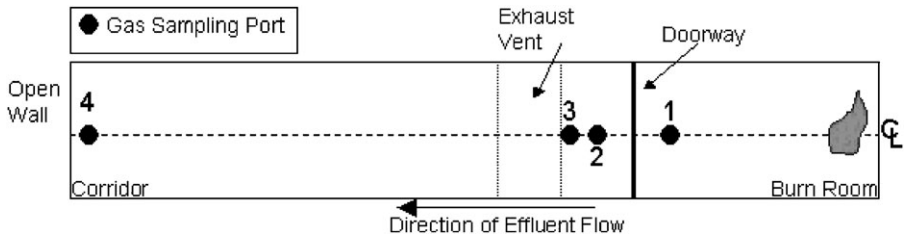


Figure 1. Schematic of the room–corridor test fixture.

Figure 2. Photograph of the room–corridor text fixture.

*Temperature.* Vertical temperature profiles were measured at four locations as input to quantifying the exit flow from the burn room and to characterizing the smoke flow down the corridor. The first thermocouple tree was located in the burn room doorway, approximately 0.10 m from the door edge. The 10 individual thermocouples were placed at heights of 0.53, 0.68, 0.83, 0.98, 1.13, 1.28, 1.43, 1.58, 1.73, and 1.88 m from the floor. The thermocouples were an aspirated design characterized by Pitts *et al.* [12] and based on a design by Newman and Croce [13]. The shields had an outer diameter of 6.3 mm. Each shield housed a type K chromel-alumel thermocouple constructed from 0.51 mm diameter wire. A flow of 18.9 L/min (at ambient temperature) was drawn through each aspirated thermocouple by a dedicated pump.

Three additional trees of 12 bare-bead thermocouples were used to determine the vertical temperature stratification (1) in the burn room approximately 1 m from the doorway wall and 1 m from the adjacent side wall, (2) in the corridor 1 m from the burn room and 1 m from the adjacent side wall, and (3) in the corridor 1 m from the open end and 1 m from the side wall. These type K thermocouples, constructed from 0.25 mm diameter wire, were spaced evenly from floor to ceiling at 150 mm $\pm$ 10 mm intervals, again beginning 0.53 m from the floor. A single type K thermocouple was located just below the centerline of the doorway lintel to assist in anticipating the onset of flashover during the tests.



DOI: 10.1002/fam

Figure 3. Photograph of four-probe effluent sampling array.

In a past series of well-controlled gas burner tests [14], the standard uncertainty for peak gas temperature had been found to be ±16°C (standard deviation of the peak values for 12 replicate tests). Random variation in the current experiments was expected to be comparable to these values.

*Velocity.* Ten bi-directional velocity probes based on a design developed by Heskestad [15] were placed at the same locations as the thermocouples in the doorway. The differential pressure from the two sides of the probes allows direct calculation of velocity and vent flow [16]. Standard uncertainty in vent flow measurements has been reported to be approximately ±10% [16].

*Combustion product sampling.* In each test, gases and soot were sampled at some or all of four locations, numbered as in Figure 1. The probes and locations were as follows.

1. Single probe, 1 m inside the burn room door, inserted through the ceiling, for sampling $CO_2$, CO, and $O_2$. For the tests with the burn room door closed, room gas was extracted from a similar, adjacent port for analysis using a Fourier transform infrared (FTIR) spectrometer.
2. Four-probe array, 1 m outside the burn room doorway (Figure 3 and Table I). This location was selected to be in the quenched doorway jet at a location where minimal dilution of the combustion products would have occurred after leaving the burn room. However, for the more intense fire stages, the flames were not always quenched at this location.
3. Single probe, 2.1 m downstream from the burn room doorway. The purpose of measurement at this location was to characterize the composition of the fixed gases just before they reached the exhaust vent.
4. Four-probe array, 9.4 m from the burn room door or approximately 1 m upstream from the open end of the corridor. This location was selected in order to be as far down the corridor as possible, yet minimize edge effects at the end of the corridor.

The tips of the 12.7 mm o.d. stainless steel probes were located on the corridor/burn room centerline, ca. 0.3 m from the ceiling, with the intent to avoid sampling from within a stagnant boundary layer, but still capture combustion products from early, low-momentum effluent flows. The tips of the probes were simply the blunt ends of the tubing. The probes at the three corridor locations were inserted horizontally through the corridor sidewall and were thus roughly isothermally heated



DOI: 10.1002/fam

Table I. Functionality of the four-probe sampling arrays.

| Probe designation | Probe location | Function |
|---|---|---|
| T | Top | Pre-flashover soot |
| B | Bottom | Post-flashover soot |
| U | Upstream | FTIR analysis |
| D | Downstream | $CO_2$, CO, and $O_2$ |

along their length to the upper layer height temperature at the time. The probes in the four-probe arrays were parallel, their tips forming a diamond 100 mm high and wide. The probe functions are described in Table I.

On the outside of the burn room or corridor wall, each probe D was connected to a length of unheated copper tubing 6.2 mm in outer diameter. Approximately 5 m downstream, this tubing was formed into a helical coil, which was immersed in an ice bath and then a dry ice bath to trap water vapor, aerosols, and soot. A length of plastic tubing continued to the analyzers. A pump located on the downstream end of the train drew sample at an estimated rate of 10 L/min.

The probes for FTIR samples (U) were connected to two polytetrafluoroethylene transfer lines 12.7 mm in outer diameter. From each of the two probes, a line, ca. 8 m in length, went directly to one of the two FTIR spectrometers. These lines were heated to 170°C to prevent the condensation of water, soot, and other nonvolatiles. There were no soot filters in the transfer lines since these also collect acid gases. While the acid gases can be extracted and analyzed after the test is over, one only obtains an integrated mass of each acid gas, and meeting the objective of this study required time-resolved (at least pre- vs post-flashover) concentration information. The flows to the FTIR spectrometers were maintained at $10 \pm 0.5$ L/min using rotameters with control valves. These flows were measured prior to each test with a dry test meter.

*Combustion product measurement.* CO and $CO_2$ concentrations were measured continuously using nondispersive infrared (NDIR) analyzers. Oxygen measurements were made using paramagnetic analyzers. None of the other combustion gases known to interfere with these measurements were expected to be present in sufficient quantity in these experiments to warrant correction to the data. Prior to each test, flows of gas mixtures of known concentration enabled any corrections to manufacturer-supplied calibration curves. Typically, these corrections were less than 1% of the measured value. For a series of well-controlled gas burner tests [14], the standard uncertainties for $O_2$, CO, and $CO_2$ concentrations were found to be $\pm 0.6\%$, $\pm 0.4\%$, and $\pm 0.06\%$, respectively. These are expressed as the standard deviation of the peak values for 12 replicate tests.

Two Midac Illuminator FTIR spectrometers equipped with mercury cadmium telluride detectors were used to measure continuously the infrared absorbance spectra of fire gases. The unit used to monitor the fire gases at Location 2 was configured with a closed optical path through an internal stainless steel cell fitted with ZnSe windows. The other spectrometer, which was used predominately at Location 4, but was moved to Location 1 for two tests, was an open path unit consisting of separate source and detector modules. An external monel cell with KBr windows was positioned in the optical path between the two modules. Although both cells were nominally 100 mm long, their optical pathlengths, which were determined by fitting the measured spectrum of CO at a known concentration to calibration spectra, were significantly different. The pathlength of the stainless steel cell with ZnSe windows was found to be 82 mm, while the monel cell with KBr windows was 115 mm. The scanning rate of both spectrometers at 0.5 $cm^{-1}$ resolution was ca.



DOI: 10.1002/fam

1.5 spectra/s. The spectrometer at Location 2 was programmed to signal average over 2 spectra, whereas the spectrometer at Location 4 was configured to signal average over 4 spectra. Therefore, the concentrations of the target compounds at Locations 2 and 4 were updated every 1.3 and 2.7 s, respectively.

In selecting cell sizes for these spectrometers, there were two conflicting considerations. A multi-pass cell with a long optical path (ca. 1 m) offers higher sensitivity, a benefit when examining trace compounds, but a problem when quantifying major species, because too little radiation reaches the detector. Furthermore, the presence of soot, which was not filtered in order to prevent toxicologically important gases from condensing, would invariably ruin the multi-path optics.** In addition, a cell with a smaller volume and short path length offers better time resolution than a longer pathlength cell, which typically has greater volume, an important issue when the combustion conditions in the fire are likely to be changing during a test. In the final analysis, durability and time resolution were higher priorities than analytical sensitivity, and the decision was to use a short path optical cell.

The toxicants under investigation were $CO_2$, CO, HCN, HCl, HF, HBr, NO, $NO_2$, $CH_2O$ (formaldehyde), and $CH_2=CH-CH=O$ (acrolein). The relative concentrations of these compounds were determined from IR absorbance measurements of the fire gases using Autoquant 3.11, a software package based on a Classical Least Squares (CLS) algorithm [17]. Calibration spectra corresponding to the IR absorbencies of known concentrations of the target compounds, and using the same optics, were obtained from Midac [18] and from Federal Aviation Administration staff who had performed bench-scale fire tests on similar materials [19]. The concentrations of CO and $CO_2$ were checked routinely using calibration mixtures.†† Non-linear dependences of absorbance on concentration were determined with an interpolation algorithm [20]. The identities of the target compounds (as well as other compounds that absorb at the same frequencies), their calibration concentrations, and the characteristic spectral windows used in the quantitative analyses are listed in Table II. Also listed in this table are minimum detection limits (MDLs) for each of the target compounds. These values, which represent the lowest concentrations that can be measured with the instrumentation employed in these tests, were estimated as follows. The calibration spectra were added to test spectra with varying coefficients until the characteristic peaks of the target compounds were just discernible above the baseline noise. The value of signal averaging over ca. 100 spectra was included. The MDL values reported in Table II were obtained by multiplying these coefficients by the known concentrations of the target compound in the calibration mixtures. Water, methane, and acetylene were included in the quantitative analyses because they have spectral features that interfere with the target compounds. The nitrogen oxides absorb in the middle of a water band. Consequently, the limits of detection for these compounds are an order of magnitude higher than for any of the other target compounds. Thus, it is not surprising that their presence was not detected in any of the tests.

Delay times for gas flows from sampling locations within the test structure to the NDIR and FTIR gas analyzers were determined by introducing a pulse of gas into the sampling lines (Table III). Calculations for several of the experiments with changes in the delays ranging from 10 to 40 s show less than 1% change in calculated species yields.

**To ensure that the cell optics had not been fouled by smoke deposits, the voltage of the interferogram was measured prior to every test to ensure adequate throughput.

††Nonlinearities were observed at high concentrations of CO and $CO_2$. In those cases, the concentrations were corrected by curve fitting. Multiple spectra were used for some analytes to mitigate any resulting inaccuracies.



DOI: 10.1002/fam

Table II. Calibration spectra for FTIR spectroscopy.

| Compound | Concentration (μL/L) | Temperature (K) ($P = 101.3$ kPa) | Frequency windows ($cm^{-1}$) | Minimum detection limit (μL/L) |
|---|---|---|---|---|
| $C_2H_2$ | 39 | 170 | 3190–3420 | — |
| $C_3H_4O$ | 225 | 100 | 850–1200<br>2600–2900 | 10 |
| $CH_4$ | 48, 422 | 170 | 2800–3215 | |
| $COH_2$ | | 100 | 2725-3000 | 50 |
| CO | 51, 241, 1460, 8977, 17 650 | 170 | 2010–2250 | 10 |
| $CO_2$ | 4785, 9125,<br>16 329 | 170 | 715–724<br>2250–2400 | 5 |
| $H_2O$ | 10 000 | 170 | 1225–2150<br>3400–4000 | — |
| HBr | 226 | 170 | 2400–2800 | 50 |
| HCN | 51, 115 | 170 | 710–722<br>3200–3310 | 50 |
| HCl | 987 | 170 | 2600–3100 | 15 |
| HF | 2025 | 170 | 4000–4150 | 5 |
| NO | 512 | 121 | 1870–1950 | 500 |
| $NO_2$ | 77 | 121 | 1550–1620 | 100 |

Table III. Instrument delay times and standard deviations (s).

| | Sampling location | | | |
|---|---|---|---|---|
| Analyzer | 1 | 2 | 3 | 4 |
| $CO_2$, CO, $O_2$ | 20±2 | 34±3 | 21±1 | 9±1 |
| FTIR | 3.0±0.5 | 2.5±0.5 | — | 3.0±0.5 |

Two samples of soot were collected at each location in each experiment: one during the pre-flashover phase and one post-flashover. At the outside of the corridor wall, each soot probe passed through a 0.42 m long water jacket heated to 55°C to prevent the condensation of water and other volatiles. The smoke was collected on a PTFE filter with a 2 μm pore size housed in a stainless steel filter holder also heated to 55°C. The collection efficiency for this filter was at least 96% for particle sizes of 0.035 μm and larger. This size range includes essentially all the smoke particles. The flow through the filter was 0.050 L/s. Additional smoke deposited on the inside of the tube was collected using a cotton pad. This fraction of the total smoke varied from about 15% for the bookcase fires to as large as 75% for the tests involving bookcases plus a PVC sheet. The smoke still remaining on the tube walls was estimated to be no more than 15% of the total. Repeat weighings of the collected smoke were made after storing the filters overnight to assess the impact of condensables. The change in mass was typically less than 2%. The typical uncertainty in the filter weighing was about 0.05 mg for a 1 mg filter weight. The filter weights ranged from 0.4 to 40 mg. The mass concentration of smoke, corrected to 101 kPa and 25°C, ranged from 0.2 to $20\,g/m^3$.

*Video.* The progress of the tests was monitored using two Super 8 video cameras. One was located beyond the open end of the corridor and viewed the full length of the corridor and the



DOI: 10.1002/fam

interior of the burn room. The second was located in the forward lower corner of the burn room and was directed upward toward the burning fuel. For the two tests where the sofas were located in the burn room center facing toward the rear, this camera was relocated to the lower rear corner. For the tests with the burn room door closed, only the second camera was used.

*Additional data*. The building temperature, pressure, and relative humidity were recorded at the beginning of each test. The time of flashover was estimated from the ignition of crumpled newspaper on the floor of the burn room and the readings from a Gardon-type total heat flux gauge whose measuring surface was flush with the floor surface of the burn room, centered between the two side walls at approximately 1 m from the doorway.

*Data collection.* The signals from the various measurement devices (except the FTIR spectrometers) were sampled at a rate of 200 scans/s. The 200 values for each channel were averaged for an overall output and storage rate of 1 sample/s. Three channel markers were used to log the times for igniting and extinguishing the pilot burner and extinguishing the fire at the end of the test, initiating and ending the pre-flashover sampling period, and the times for the occurrence of flashover and the beginning and ending of the post-flashover sampling period.

*Ignition.* Three ignition sources were used in the test series. The propane burner in California Technical Bulletin 133 [21] was used for the sofa and bookcase tests. It consists of a perforated square 'ring' with an outer dimension of 0.25 m attached to a supply tube at the center of one side of the square. The electrical cable was ignited using two 152 mm square sand-filled propane burners connected at the centers of their bottoms by a 12.7 mm steel pipe. A loop of nichrome heater wire inserted into a book of matches was used to ignite the fires in the closed compartment tests.

### *2.3. Combustibles*

Four fuels were selected for diversity of physical form, combustion behavior, and the nature and yields of toxicants produced. Specimens of the principal components of each fuel were sent to an independent testing laboratory to characterize their chemical nature; the oxygen content was estimated using the empirical formulae of the compounds. The test configurations were selected to provide burning durations (under both pre-flashover and post-flashover conditions) that were long enough for substantive combustion product analyses. In some cases, adherence to realism was sacrificed to achieve this.

- *'Sofas' made of up to 14 upholstered cushions supported by a steel frame.* A 0.46 m × 0.46 m × 0.15 m cushion consisted simply of a zippered cotton-polyester fabric over a block of foam. The elemental content of the cushions was, by mass, 54.5%C, 8.0% H, 10.0% N, 0.68% Cl, 0.15% P, and ca. 26.7% O. The mass of a cushion was about 1.1 kg, and the heat of combustion was 24.4 MJ/kg ±2.7%. The California TB133 propane ignition burner faced downward, centered over the center of the sofa, about 0.1 m above the top surface of the cushions. In all but two of the tests, the sofa was centered along the rear wall of the burn room facing the doorway. Two of the sofa tests were in a closed room to examine the effect of vitiation.
- *Particleboard* (*wood with urea formaldehyde binder*) *bookcases with a laminated vinyl finish.* The bookcases were 1.83 m high × 0.91 m wide × 0.30 m deep. The back of the bookcase was a sheet of vinyl-laminated pressboard. The bookcase mass was ca. 27.5 kg. A diagonal length of steel angle iron was attached to the rear of the bookcases to prevent buckling and falling off the load cell during the test. The chemical analyses of the bookcases indicated a composition of 48.1%C, 6.2%H, 2.9%N, 0.3%Cl, and 42.6%O. The heat of combustion was



DOI: 10.1002/fam

18.2 MJ/kg ± 0.4%. Early experiments with two bookcases side by side and the burner in between failed to sustain burning. As a result, two bookcases were placed in a 'V' formation, with the TB133 burner facing upward approximately 0.30 m under the lower shelves and 0.30 m from the back of the 'V.'

- *Rigid polyvinyl chloride* (*PVC*) *product sheet* (*a window frame material*). Each test involved a single horizontal sheet of unplasticized PVC that was 0.71 m × 1.83 m × 7.9 mm in the room with burning bookcases. The elemental composition of the combustible portion of the sheet was 42.3%C, 5.53%H, and 52.2%Cl. The measured heat of combustion was 16.2 kJ/kg ± 1.0%.
- *Household wiring cable*, *consisting of two 14 gauge copper conductors insulated with nylon and PVC*, *an uninsulated ground conductor*, *two paper filler strips, and an outer jacket of plasticized PVC.* The fuel composition was 45.8%C, 6.2%H, 1.62%N, 25.2%Cl, and ca. 20%O. The heat of combustion for the combustible fraction of the cable was 21.6 MJ/kg ± 0.6%. To determine the size of the cable array needed to bring the burn room to flashover and to sustain post-flashover burning for about 3 min, we used data from Dey [22]. Two 1.83 m long cable racks containing three trays each were constructed, with 30 kg of cable in each of the bottom two trays and 17 kg in each of the middle and top trays. The cable trays were placed parallel to the rear of the burn room. The twin propane ignition burners were centered under the bottom tray of each rack.

Supplies of each of the test fuels were stored for future use in bench-scale test method assessment.

### *2.4. Experiments performed*

Preliminary experiments established the ignition protocol, determined the mass of fuel needed to produce flashover, and scoped the rates of mass loss. A series of 23 tests were then conducted. The data from some were not usable due to instrument malfunction, etc.

The key to the test designations, XYZn, is as follows:

X: Fuel [S = sofas; B = bookcases; P = power cable]
Y: Q = heat release rate test, added to the key only when the ceiling hole was open
Z: W = combustibles located near rear wall of burn room
C = doorway closed
P = PVC sheet included
n: test number for that set of combustibles and location

The following comprise the tests analyzed here. Figures 4–7 depict the specimen configurations.

- Three tests with an 8- or 12-cushion sofa (SW1 through SW3). These tests did not reach flashover, but generated additional data for pre-flashover conditions.
- Five replicate tests with a 14-cushion sofa located against the back wall of the burn room, facing the open doorway (SW10 through SW14). The intent was to provide an estimate of test repeatability.
- Two tests with the sofa against the back wall, but with the doorway sealed, to determine the effect of room vitiation (SC1 and SC2).
- Six tests of two bookcases each (BW2 through BW7). There were no FTIR measurements in BW2, BW3, BW5, and BW6.
- Three similar bookcase tests with the rigid PVC sheeting product (BP1 through BP3).



DOI: 10.1002/fam

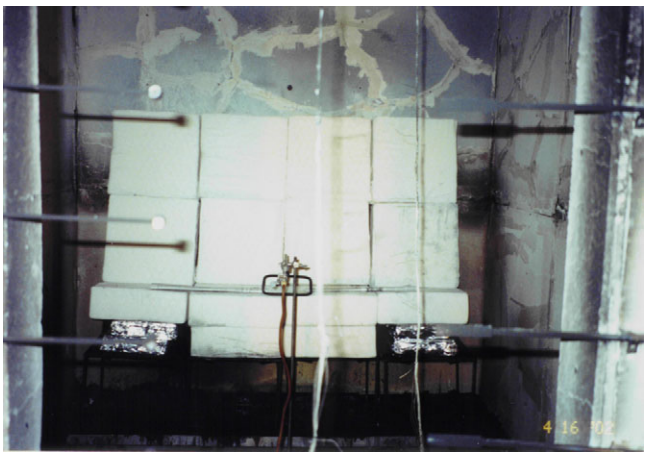

Figure 4. Photograph of a 14-cushion Sofa.

Figure 5. Photograph of an 8-cushion Sofa.

- Four tests of electric cable in the tray assembly (PQ1, PQ2, PW1, and PW2). In two of these tests, the vent was opened in the ceiling of the corridor to collect the effluent for heat release rate measurements.

Data were collected continuously during a test, beginning with instrument calibration and followed by a quiescent 'zeroing' interval. The appropriate burner was then lit and applied to the combustible until there were sustained flames over a volume distinctly greater than the burner flame. At that point, the burner was extinguished. Pre-flashover effluent was then measured to the point where flashover was approaching. The post-flashover data interval continued for 3 min



DOI: 10.1002/fam

Figure 6. Photograph of bookcases in the burn room.


Figure 7. Photograph of cable trays in the burn room.

or until the time when the combustion became fuel-limited and reverted to non-flashover burning conditions. The closed-door tests did not reach flashover and self-extinguished, presumably due to a lack of oxygen.



DOI: 10.1002/fam

## 3. CALCULATION METHODS

The mass loss rates were determined from the slopes of the plots of mass vs time. The noise in the instantaneous measurements was reduced using a running seven-point linear regression of the mass loss data. The measurement uncertainty was derived from the linearity and sensitivity limit of the load cell.

The uncertainty in the doorway flow measurements is significant. Since the pressure drop across an opening passes through zero as the flow changes direction at the height of the neutral plane, measurement of the velocity profile in a doorway is particularly difficult. Estimation of the pressure in the extreme lower resolution of the instrumentation (as the pressure drop approaches zero) adds to the uncertainty of the measurement. For the same range of experiments noted above for heat release rate, the repeatability of the vent mass flow calculation averaged 35% [23]. The measurement uncertainty in the current experiments is expected to be comparable to this.

The fuel to air global equivalence ratio is defined as:

$$\frac{\dot{m}_{\text{fuel}}/\dot{m}_{\text{air}}}{[\dot{m}_{\text{fuel}}/\dot{m}_{\text{air}}]_{\text{stoichiometric}}}$$

where $\dot{m}_{\text{fuel}}$ is the gasification rate of the combustible and $\dot{m}_{\text{air}}$ is the total flow into the burn room. The uncertainty in the equivalence ratio is the sum of the uncertainties in the mass loss rate, the doorway flow, and the empirical formula.

The notional, or maximum possible, gas yields (Table IV) were calculated assuming that all the carbon in the test specimen was converted to $CO_2$, CO, or HCN and that all the chlorine was converted to HCl. The uncertainty in the notional yield values was determined by the uncertainty in the prevalence of the central element in the combustible.

The uncertainties in the NDIR concentrations were below 1% of the measured values. The volume fraction limit of detection was about $1 \times 10^{-5}$ for both the CO and $CO_2$ analyzers. There was a considerable range of uncertainties in the concentrations measured using FTIR due to variation in the closeness of the signal to the background level and the degree of spectral interference from other species. The uncertainty in the $CO_2$ volume fractions was generally less than $\pm 1\%$ at both Locations 2 and 4 and for both pre- and post-flashover measurements. The exceptions were for test SW13, pre-flashover, at Location 2, where the uncertainty was $\pm$ 10% and for tests SW11 and SW12, pre-flashover, at Location 4 where the uncertainty was $\pm 3\%$.

The general uncertainties in the FTIR-measured CO, HCl and HCN volume fractions and the exceptions are noted in Table V.

The pre- and post-flashover yields of $CO_2$ calculated by integrating the mass of each gas of interest flowing through the doorway over the corresponding time interval and normalizing by the total mass loss. The yields of the other gases were obtained by multiplying the ratio of the mass

Table IV. Estimated notional yields of toxic products (mass fraction).

| | Bookcase | Sofa | PVC sheet | Cable |
|---|---|---|---|---|
| $CO_2$ | 1.72 | 2.00 | 1.55 | 2.11 |
| CO | 1.09 | 1.27 | 0.98 | 1.33 |
| HCN | 0.057 | 0.193 | — | 0.040 |
| HCl | 0.0026 | 0.0070 | 0.537 | 0.332 |



DOI: 10.1002/fam

Table V. Unusual/large uncertainties (% of value) in FTIR measurements.

| | Pre-flashover | | | | | | Post-flashover | | | | | |
|---|---|---|---|---|---|---|---|---|---|---|---|---|
| | Location 2 | | | Location 4 | | | Location 2 | | | Location 4 | | |
| Test | CO | HCl | HCN | CO | HCl | HCN | CO | HCl | HCN | CO | HCl | HCN |
| Gen'l | ±10 | ±20 | ±20 | ±10 | ±25 | ±25 | ±1 | ±5 | ±10 | ±5 | ±25 | ±25 |
| SW1 | | | | | ±44 | ±44 | | | | | | |
| SW2 | | | | | | ±209 | | | | | | |
| SW3 | | | | | ±162 | ±162 | | | | | | |
| SW10 | | | | ±26 | | | | | | | | |
| SW11 | ±76 | | | ±24 | ±85 | ±194 | | | | ±25 | | |
| SW12 | | | ±32 | ±218 | ±44 | ±51 | | | | ±28 | | ±32 |
| SW13 | | ±125 | | ±151 | ±28 | ±378 | | | | ±316 | ±32 | |
| SW14 | | | | ±16 | ±75 | ±213 | | | | ±100 | | |
| BW7 | | | | ±17 | ±34 | | | | | | | |
| BP1 | | ±147 | | | ±65 | | | | | ±17 | ±112 | |
| BP2 | | | | | ±93 | | | | | ±24 | | ±30 |
| BP3 | | | | | | ±130 | | | | | | |

fraction of toxicant in the flow stream to that of $CO_2$ by the yield of $CO_2$. The uncertainties were obtained as the standard deviations of the least squares fits of the calibration to the test spectra.

For the closed-room tests, we assumed that the upper gas layer in the room was well mixed. The measured volume fractions of the gases and the ideal gas law were used to calculate the mass of each species in the upper layer. These were normalized to specimen mass loss, as a function of time. The uncertainty in the yields can be further estimated by comparing the values from the early combustion with those from the pre-flashover segments of the open door sofa tests.

For the PVC sheets, only post-flashover results were possible, since the mass loss was negligible before flashover. It was assumed that all the HCl was from the PVC sheet and that all the HCN came from the bookcases. Since the scatter in the CO and $CO_2$ yields was comparable to any differences between tests with and without the PVC sheet, yield data for these two gases from the PVC sheet itself were not calculable.

The uncertainty in a yield value results from the sensitivity of the yield to the selected pre- or post-flashover time interval, the uncertainty in the specimen mass loss, the uncertainty in the species mass flow out the doorway (for open door tests), and the quality of the assumptions inherent in the calculation of the mass of product in the upper layer (for closed room tests). For the closed room tests, the uncertainty was further estimated by comparing the yield values from the early combustion with those from the pre-flashover segments of the open door sofa tests. The analysis of similar tests also structured the determination of uncertainty and repeatability.

Some of the data were not used because an instrument malfunctioned, the upper layer (containing the combustion products) did not fully envelop the sampling probe tips, or the concentration values were too close to the background levels.

The smoke yield was determined by the carbon balance method. The equation for calculating smoke yield, $y_s$, as expressed in terms of $CO_2$ and CO concentrations, is:

$$y_s = \frac{f m_s}{[m_s + 12 n_t (X_{CO} + X_{CO_2}]}.$$



DOI: 10.1002/fam

The quantity $f$ is the mass fraction of carbon in the combustible, $m_s$ is the mass of the smoke sample collected on a filter, $n_t$ is the number of moles of air sampled, $X$ is the volume fraction of the gas identified in the subscript, and the constant 12 represents the molar mass of carbon in grams. The other carbon-containing gases were neglected, a good approximation for overventilated burning. However, for underventilated burning, incompletely burned hydrocarbons could account for as much as 20% of the carbon [24]. The assumption that the smoke mass is all carbon could lead to an underestimate of the yield by no more than 1%.

## 4. RESULTS

### *4.1. Test data*

The calculated yields of CO, $CO_2$, HCl, and HCN from Location 2 measurements in the open room tests are compiled in Table VI. During the test sequence, there were occasions where instruments did not function properly. The following summarizes those cases and any actions taken to salvage the experiment.

- SW11: Velocity probes at 0.98 and 0.83 m from the floor and doorway temperature measurement at 1.58 m from the floor failed. Doorway flows were calculated from operating doorway velocity and temperature instruments.
- SW13: Load cell 'stuck' during pre-flashover period (low mass loss). The mass loss was set equal to the mean from tests SW10, SW11, SW12, and SW14.
- SW14: Load cell 'stuck' during pre-flashover period (low mass loss). The pre-flashover mass loss rate was estimated from mean mass loss of SW1-SW3 and SW10-SW13.
- BW7: Location 1 sampling failed during post-flashover period. The data were discarded.
- BP2: The load cell under the PVC sheet failed. We used a substitute PVC mass loss curve from test BP1, normalized by the ratio of the mass loss curves from the main load cell.
- BP2: The filter on the $CO/CO_2$ sampling train at Location 2 partially clogged during the post-flashover period. Post-flashover NDIR gas concentrations were shifted by 30 s to correlate with the downstream data.
- BP3: The PVC load cell and the Location 1 sampling train failed. We used a substitute PVC mass loss curve from test BP1, normalized by the ratio of the mass loss curves from the main load cell.
- PW2: Load cell failed. We adjusted the PW2 mass loss rate such that the $CO_2$ yield equaled that from test PW1.

Tests SW1, SW2, and SW3 did not go to flashover. Other blank cells indicate data that would have had to be derived from an uninstalled or non-functioning analyzer. A pound sign ($^{\#}$) indicates data that have been reconstructed as noted above. An asterisk ($^{*}$) marks data derived from sampling that was not assuredly from the upper layer or for which the signal was too close to the background.

The yields of the same four gases from the closed door tests are compiled in Table VII. Since the gases were accumulated within the room, it was possible to calculate the evolving time-averaged yields of these gases as the test progressed. Note that the early NDIR yields for $CO_2$ and CO were close to those for the open door sofa tests. As the fire progressed, the $CO_2$ yield decreased and the CO yield increased, as expected from burning in an increasingly vitiated atmosphere.



DOI: 10.1002/fam

Table VI. Yields of combustion products for open room tests.

| | Pre-flashover | | | | | | Post-flashover | | | | | |
|---|---|---|---|---|---|---|---|---|---|---|---|---|
| | CO | $CO_2$ | CO | $CO_2$ | HCl | HCN | CO | $CO_2$ | CO | $CO_2$ | HCl | HCN |
| Test↓ | NDIR | NDIR | FTIR | FTIR | FTIR | FTIR | NDIR | NDIR | FTIR | FTIR | FTIR | FTIR |
| SW1 | 2.20E–02 | 1.54$E$+00 | 1.73E–02 | 1.78$E$+00 | 1.38E–02 | 4.28E–03 | | | | | | |
| SW2 | 9.26E–03 | 1.06$E$+00 | 9.34E–03 | 1.49$E$+00 | 1.52E–02* | 1.24E–03* | | | | | | |
| SW3 | 1.32E–02 | 1.32$E$+00 | 1.55E–02 | 2.06$E$+00 | 2.57E–02* | 4.95E–03* | | | | | | |
| BW2 | 4.67E–03 | 9.89E–02 | | | | | | | | | | |
| BW3 | 1.51E–03 | 5.35E–02 | | | | | 5.63E–02 | 8.80E–01 | | | | |
| BW4 | 1.18E–02 | 4.14E–01 | 4.14E–03 | 2.46E–01 | 5.45E–04* | 4.29E–04* | 2.78E–01 | 4.69$E$+00 | 5.26E–02 | 1.30$E$+00 | 7.51E–04 | 3.63E–03 |
| BW5 | 1.28E–02 | 4.83E–01 | | | | | | | | | | |
| BW6 | 4.71E–02 | 5.80E–01 | | | | | 3.72E–02 | 5.71E-01 | | | | |
| PQ1 | 4.67E–03 | 7.86E–02 | 3.10E–04 | 1.00E–02 | 4.97E–05* | 1.58E–04* | 1.48E–01 | 1.30$E$+00 | 1.82E–01 | 1.51$E$+00 | 2.31E–01 | 5.95E–03 |
| PQ2 | 1.09E–02 | 2.04E–01 | 6.29E–03 | 1.91E–01 | 6.00E–03 | 5.73E–04* | 1.15E–01 | 1.07$E$+00 | 1.29E–01 | 1.16$E$+00 | 1.72E–01 | 3.24E–03 |
| PW1 | 6.82E–03 | 1.06E–01 | 3.18E–03 | 8.17E–02 | 9.57E–03 | 3.09E–04 | 1.51E–01 | 1.33$E$+00 | 1.55E–01 | 1.62$E$+00 | 2.16E–01 | 3.12E–03 |
| PW2 | 2.94E−03# | 1.06E−01# | 3.60E−03# | 7.49E−02# | 4.34E−03# | 1.01E−03# | 1.50E–01 | 1.33$E$+00 | 1.56E–01 | 1.70$E$+00 | 2.20E–01 | 3.85E–03 |
| SW10 | 6.54E–04 | 7.03E–02 | 4.61E–04 | 2.85E–02 | 4.86E–04* | 3.76E–04* | 5.87E–02 | 1.11$E$+00 | 5.75E–02 | 1.06$E$+00 | 5.47E–03 | 1.86E–02 |
| SW11 | 3.13E–03 | 2.77E–01 | 4.61E–04 | 1.86E–01 | 2.95E–03* | 1.55E–03* | 3.37E–02 | 7.75E–01 | 2.64E–02 | 7.84$E$+01 | 5.53E–03 | 8.36E–03 |
| SW12 | 1.06E–03 | 2.06E–01 | 8.16E–04 | 9.32E–02 | 1.08E–03* | 1.81E–04* | 5.28E–02 | 9.53E–01 | 5.54E–02 | 1.21$E$+00 | 4.89E–03 | 1.72E–02 |
| SW13 | 2.24E−04# | 2.23E−02# | 3.84E−04# | 5.78E−02# | 1.14E−04#* | 3.42E−04#* | 5.45E–02 | 1.27E+00 | 4.55E–02 | 1.14$E$+00 | 9.73E–03 | 1.66E–02 |
| SW14 | 4.55E−03# | 9.97E−02# | 9.98E−04# | 4.60$E$−02# | 6.89E−04#* | 2.79E−04#* | 6.62E–02 | 1.35$E$+00 | 5.92E–02 | 1.65$E$+00 | 4.22E–03 | 1.64E–02 |
| BP1 | 2.31E–03 | 1.53E–01 | 8.89E–04 | 4.69E–02 | | 7.76E–05* | 4.49E–02 | 6.25E–01 | 3.17E–02 | 2.77E–01 | 1.67$E$+00 | 3.63E–01 |
| BP2 | 4.11E–02 | 1.05$E$+00 | 4.51E–02 | 1.85$E$+00 | 6.58E−03#* | 3.33E–03* | 7.87E–02 | 2.09$E$+00 | 3.00E–02 | 4.67E–01 | 4.87$E$+00# | 5.12E–01 |
| BW7 | 2.30E–02 | 5.41E–01 | 2.43E–02 | 1.01$E$+00 | 3.76E–03 | 4.99E–04* | 5.74E–02 | 2.35$E$+00 | 2.52E–02 | 1.53$E$+00 | 3.63E–03 | 1.36E–03 |
| BP3 | 6.65E–03 | 2.49$E$+00 | 6.66E–03 | 3.98E–01 | 9.90E−04# | 3.49E–04* | 5.26E–03 | 2.42E–01 | 6.04E–03 | 1.87E-01 | 2.58E−01# | 4.06E–04 |




DOI: 10.1002/fam

Table VII. Yields of combustion products from closed room tests.

| Time (s) | Volume fraction | | | | | | Mass lost (kg) | Upper layer depth (m) | Mean upper layer T (K) | Yield | | | | | |
|---|---|---|---|---|---|---|---|---|---|---|---|---|---|---|---|
| | NDIR | | FTIR | | | | | | | NDIR | | FTIR | | | |
| | $CO_2$ | CO | $CO_2$ | CO | HCl | HCN | | | | $CO_2$ | CO | $CO_2$ | CO | HCl | HCN |
| SC1 | | | | | | | | | | | | | | | |
| 150 | 3.60E–02 | 5.10E–04 | 2.40E–02 | 2.02E–04 | 7.50E–07 | 2.60E–06 | 0.44 | 1.85 | 498 | $1.45E+00$ | 1.31E–02 | 9.65E–01 | 5.17E–03 | 2.43E–05 | 6.42E–05 |
| 200 | 6.13E–02 | 1.20E–03 | 3.90E–02 | 3.74E–04 | 2.20E–06 | 7.70E–05 | 0.84 | 1.85 | 493 | $1.31E+00$ | 1.64E–02 | 8.36E–01 | 5.10E–03 | 3.80E–05 | 1.01E–03 |
| 250 | 7.80E–02 | 2.53E–03 | 5.04E–02 | 7.00E–04 | 1.54E–06 | 1.91E–04 | 1.17 | 1.85 | 488 | $1.21E+00$ | 2.50E–02 | 7.83E–01 | 6.92E–03 | 1.93E–05 | 1.82E–03 |
| 300 | 8.61E–02 | 4.15E–03 | 5.95E–02 | 1.19E–03 | 2.67E–05 | 2.79E–04 | 1.40 | 1.85 | 473 | $1.15E+00$ | 3.54E–02 | 7.97E–01 | 1.01E–02 | 2.89E–04 | 2.29E–03 |
| 350 | 8.75E–02 | 5.66E–03 | 4.60E–02 | 1.82E–03 | 4.50E–05 | 3.37E–04 | 1.60 | 1.85 | 443 | $1.10E+00$ | 4.51E–02 | 5.76E–01 | 1.45E–02 | 4.54E–04 | 2.59E–03 |
| 400 | 8.14E–02 | 5.40E–03 | 4.10E–02 | 1.64E–03 | 3.90E–05 | 3.00E–04 | 1.70 | 1.85 | 435 | 9.77E–01 | 4.12E–02 | 4.92E–01 | 1.25E–02 | 3.78E–04 | 2.21E–03 |
| 450 | 7.68E–02 | 5.20E–03 | 5.85E–02 | 1.62E–03 | 4.82E–05 | 2.89E–04 | 1.76 | 1.85 | 408 | 9.49E–01 | 4.09E–02 | 7.23E–01 | 1.27E–02 | 4.81E–04 | 2.19E–03 |
| 500 | 7.09E–02 | 4.80E–03 | 5.18E–02 | 1.57E–03 | 4.35E–05 | 2.60E–04 | 1.83 | 1.85 | 403 | 8.53E–01 | 3.67E–02 | 6.23E–01 | 1.20E–02 | 4.22E–04 | 1.92E–03 |
| SC2 | | | | | | | | | | | | | | | |
| 150 | 2.90E–02 | 4.20E–04 | 1.06E–02 | 7.60E–05 | 1.33E–05 | 3.34E–07 | 0.24 | 1.75 | 463 | $2.19E+00$ | 2.02E–02 | 8.01E–01 | 3.65E–03 | 8.10E–04 | 1.55E–05 |
| 200 | 5.33E–02 | 9.90E–04 | 2.17E–02 | 1.75E–04 | 8.50E–05 | 7.50E–06 | 0.62 | 1.85 | 488 | $1.56E+00$ | 1.85E–02 | 6.36E–01 | 3.27E–03 | 2.01E–03 | 1.35E–04 |
| 250 | 7.06E–02 | 2.20E–03 | 3.05E–02 | 2.55E–04 | 1.60E–04 | 4.36E–05 | 0.92 | 1.85 | 473 | $1.44E+00$ | 2.85E–02 | 6.22E–01 | 3.31E–03 | 2.63E–03 | 5.46E–04 |
| 300 | 7.64E–02 | 3.50E–03 | 4.70E–02 | 5.60E–04 | 1.04E–04 | 1.56E–04 | 1.11 | 1.85 | 448 | $1.36E+00$ | 3.97E–02 | 8.39E–01 | 6.36E–03 | 1.50E–03 | 1.71E–03 |
| 350 | 7.71E–02 | 3.90E–03 | 5.40E–02 | 7.20E–04 | 3.70E–05 | 2.14E–04 | 1.27 | 1.85 | 438 | $1.23E+00$ | 3.96E–02 | 8.61E–01 | 7.31E–03 | 4.76E–04 | 2.09E–03 |
| 400 | 7.56E–02 | 4.05E–03 | 4.80E–02 | 9.90E–04 | 4.20E–05 | 2.32E–04 | 1.41 | 1.85 | 423 | $1.12E+00$ | 3.83E–02 | 7.14E–01 | 9.37E–03 | 5.04E–04 | 2.12E–03 |
| 450 | 7.26E–02 | 4.14E–03 | 5.67E–02 | 8.50E–04 | 4.40E–05 | 2.35E–04 | 1.49 | 1.85 | 418 | $1.03E+00$ | 3.75E–02 | 8.08E–01 | 7.71E–03 | 5.06E–04 | 2.05E–03 |
| 500 | 7.34E–02 | 4.32E–03 | 5.36E–02 | 9.70E–04 | 4.60E–05 | 2.41E–04 | 1.61 | 1.85 | 413 | 9.79E–01 | 3.67E–02 | 7.15E–01 | 8.24E–03 | 4.95E–04 | 1.97E–03 |
| 550 | 7.18E–02 | 4.35E–03 | 5.72E–02 | 9.20E–04 | 4.80E–05 | 2.50E–04 | 1.70 | 1.85 | 408 | 9.18E–01 | 3.54E–02 | 7.32E–01 | 7.49E–03 | 4.95E–04 | 1.96E–03 |
| 600 | 6.95E–02 | 4.35E–03 | 5.78E–02 | 1.03E–03 | 5.10E–05 | 2.53E–04 | 1.76 | 1.85 | 395 | 8.87E–01 | 3.53E–02 | 7.38E–01 | 8.37E–03 | 5.25E–04 | 1.98E-03 |




DOI: 10.1002/fam

Table VIII. Volume fraction ratios $[CO]_{loc4}/[CO]_{loc2}$ or $[CO_2]_{loc4}/[CO_2]_{loc2}$ and standard deviations.

| | Late pre-flashover | | Post-flashover | |
|---|---|---|---|---|
| | Location 2 | Location 4 | Location 2 | Location 4 |
| $CO_2$ | 0.71±0.11 | 1.87±0.60 | 0.97±0.19 | 0.46±0.03 |
| CO | 0.99±0.19 | 5.7±3.7 | 1.17±0.35 | 1.91±0.26 |

Table IX. Volume fraction ratios $[CO_2]_{loc4}/[CO_2]_{loc2}$ and standard deviations.

| | Late pre-flashover | | Post-flashover | |
|---|---|---|---|---|
| | Location 2 | Location 4 | Location 2 | Location 4 |
| $CO_2$ | 0.83±0.16 | 1.25±0.19 | 0.59±0.07 | 0.38±0.16 |

### *4.2. Checks on data reliability*

There are certain ratios whose values are fixed or can be estimated. Examining these provides a first assessment as to the integrity of the data set.

*4.2.1. Cross-instrument similarity.* The ratio of the CO and $CO_2$ volume fractions obtained using NDIR to those measured using FTIR should ideally be unity provided they are measured at the same location. This was essentially the case for the post-flashover values at Location 2, which represent the highest concentrations, the highest signal-to-noise ratios, and the most repeatable sampling; as expected, they best manifested proper behavior (Table VIII). The late pre-flashover data (tests SW1, SW2, and SW3) at Location 2 are nearly as good.

Much of the pre-flashover data from Location 4 were too near background to assess agreement, and the vertical temperature profiles indicated that the Location 4 sampling probes were not always safely in the hot upper layer and thus were not assuredly sampling room fire effluent. The downstream pre-flashover CO measurements approached the detection limits of the analyzers. Nonetheless, it appears that the FTIR pre-flashover CO measurements were consistently smaller than those using NDIR for reasons not yet understood. The Location 4 data were not used in further calculations.[‡‡]

*4.2.2. Location similarity.* The ratio of the volume fractions of $CO_2$ measured at two locations should reflect dilution only and thus should be the same for all tests and instruments. Table IX indicates that the two pre-flashover ratios are within experimental variability, as are the two post-flashover ratios.

[‡‡]The disagreement was not due to the NDIR measurements being for dry gases and the FTIR for wet gas. If the nominal formula of the fuel was $CH_2$, then the volume fraction of water would have been similar to the volume fraction of $CO_2$. These values were never higher than about 0.04 at Location 4. Thus, while we did not correct for this, the effect would have been minimal.



DOI: 10.1002/fam

Table X. Fractions of notional yields.

| | | $CO_2$ | CO | HCl | HCN |
|---|---|---|---|---|---|
| Sofa | Post-flashover | $0.57 \pm 0.12$ | $(4.0 \pm 0.9) \times 10^{-2}$ | $0.86 \pm 0.27$ | $(7.8 \pm 1.8) \times 10^{-2}$ |
| | Pre-flashover | $0.80 \pm 0.17$ | $(1.13 \pm 0.35) \times 10^{-2}$ | $2.6 \pm 0.8$ | $(1.81 \pm 0.83) \times 10^{-3}$ |
| | Closed (200 s)* | $0.72 \pm 0.07$ | $(1.37 \pm 0.08) \times 10^{-2}$ | $(7 \pm 1) \times 10^{-2}$ | $(1.1 \pm 0.1) \times 10^{-1}$ |
| Book-case | Post-flashover | $1.10 \pm 0.80$ | $(4.2 \pm 1.2) \times 10^{-2}$ | $0.85 \pm 0.55$ | $(4.4 \pm 2.0) \times 10^{-2}$ |
| | Pre-flashover | $0.29 \pm 0.14$ | $(2.2 \pm 1.2) \times 10^{-2}$ | $0.85 \pm 0.64$ | $(8.1 \pm 0.6) \times 10^{-3}$ |
| Cable | Post-flashover | $0.65 \pm 0.10$ | $0.111 \pm 0.013$ | $0.58 \pm 0.06$ | $0.100 \pm 0.028$ |
| | Pre-flashover | $(5.7 \pm 2.4) \times 10^{-2}$ | $(4.1 \pm 1.9) \times 10^{-3}$ | $(1.78 \pm 0.48) \times 10^{-2}$ | $(1.58 \pm 0.72) \times 10^{-2}$ |

*Earliest time with significant combustible mass loss and before significant vitiation. Calculations are for comparison with open-door pre-flashover results.

*4.2.3. Notional yield fractions.* One check on the accuracy of the measurements was to compare calculated yields with the notional or maximum possible yields (Table X). Most of the fuel carbon appears as $CO_2$, with up to ca. 20% appearing as CO and carbonaceous soot. The post-flashover notional yield fractions of $CO_2$ from all three combustibles were indeed unity or less than a factor of two lower than unity (Table X). Under pre-flashover conditions, the yields were more variable. In the closed room tests, the yield began at about the notional level, then declined to about half that as room vitiation affected the completeness of combustion.

The HCl yields were close to notional under post-flashover conditions for all the combustibles. Very low pre-flashover values for the electrical cable reflect the known HCl reaction with the calcium carbonate filler in the cable jacket. While little of the nitrogen in the combustibles generally ended up in HCN, there was an over 10% conversion from the post-flashover burning of the bookcases and cable. For HCl, a value less than unity probably represents losses to the walls combined with losses in the sampling line; the high pre-flashover value for the sofa probably reflects degradation of the chlorinated fire retardant ahead of combustion of the carbon. The values for CO and HCN should be well under unity, as most of the C and N is expected to be found in other combustion products.

### *4.3. Test repeatability*

It is well known that there are numerous sources of variability in real-scale fire tests. These could also impact the repeatability of the measured toxicant yields. Time and resources did not provide for an exhaustive evaluation of test repeatability. Table XI shows the mean yields of the principal toxicants and the standard deviation from five replicate tests (SW10 to SW14) of one fuel and configuration. Table XII shows the later pre-flashover data for tests SW1 to SW3.

### *4.4. Species losses during transport*

The data in Table XIII indicate the degree of concentration decrease during travel down the corridor.

### *4.5. Estimates of toxic gas yields with uncertainties*

Table XIV contains the yields of the combustion products calculated using the data from Location 2. The HCl yields for the three bookcase tests with a PVC sheet was $2.3 \pm 85\%$. The estimated



DOI: 10.1002/fam

Table XI. Variance in product yields among replicate tests (SW10 to SW14).

| | | $CO_2$ | CO | HCl | HCN |
|---|---|---|---|---|---|
| Pre-flashover | NDIR | $0.135 \pm 0.092$ (69%) | $(1.92 \pm 1.65) \times 10^{-3}$ (86%) | — | — |
| | FTIR | $(8.2 \pm 5.6) \times 10^{-2}$ (68%) | $(6.2 \pm 2.4) \times 10^{-4}$ (39%) | $(1.06 \pm 0.99) \times 10^{-3}$ (94%) | $(5.5 \pm 5.1) \times 10^{-4}$ (92%) |
| Post-flashover | NDIR | $1.09 \pm 0.21$ (19%) | $(5.3 \pm 1.1) \times 10^{-2}$ (21%) | — | — |
| | FTIR | $1.17 \pm 0.28$ (24%) | $(4.9 \pm 1.2) \times 10^{-2}$ (25%) | $(6.0 \pm 1.9) \times 10^{-3}$ (32%) | $(1.5 \pm 0.36) \times 10^{-2}$ (24%) |

Table XII. Variance in product yields among replicate tests (SW1 to SW3).

| | | $CO_2$ | CO | HCl | HCN |
|---|---|---|---|---|---|
| Pre-flashover | NDIR | $1.31 \pm 0.20$ (15%) | $(1.48 \pm 0.53) \times 10^{-2}$ (36%) | — | — |
| Pre-flashover | FTIR | $1.78 \pm 0.23$ (13%) | $(1.40 \pm 0.34) \times 10^{-2}$ (24%) | $(1.82 \pm 0.53) \times 10^{-2}$ (29%) | $(3.5 \pm 1.6) \times 10^{-3}$ (45%) |

Table XIII. Ratios of downstream (Location 4) to upstream (Location 2) concentrations (post-flashover data).

| | Analyzer | Sofa | Bookcase | Cable | Bookcase/PVC |
|---|---|---|---|---|---|
| $CO_2$ | NDIR | $0.65 \pm 0.05$ | $0.48 \pm 0.05$ | $0.58 \pm 0.01$ | $0.60 \pm 0.04$ |
| CO | NDIR | $0.54 \pm 0.21$ | $0.41 \pm 0.09$ | $0.57 \pm 0.02$ | $0.75 \pm 0.26$ |
| $CO_2$ | FTIR | $0.41 \pm 0.14$ | 0.73 | $0.35 \pm 0.02$ | $0.25 \pm 0.24$ |
| CO | FTIR | $0.07 \pm 0.04$ | 0.57 | $0.12 \pm 0.01$ | $0.10 \pm 0.02$ |
| HCl | FTIR | $0.08 \pm 0.05$ | $0.53 \pm 0.50$ | $0.21 \pm 0.02$ | $0.11 \pm 0.09$ |
| HCN | FTIR | $0.17 \pm 0.09$ | 0.43 | $0.45 \pm 0.02$ | $0.39 \pm 0.18$ |
| Smoke | Filter | $0.47 \pm 0.10$ | $0.45 \pm 0.22$ | $0.18 \pm 0.04$ | $0.39 \pm 0.18$ |

uncertainties reflect the repeatability of similar tests, discounting of disparate individual test results, and degree of proximity of the measured values to the background levels.

It was noticed (and is discussed in the following section) that the post-flashover CO yields were lower than expected. For that reason, we have compiled in Table XV, for the post-flashover portion of each test, an estimate of the fraction of carbon atoms appearing in CO (approximated as $[CO]/\{[CO]+[CO_2]\}$) at both Location 1 (near the ceiling of the burn room) and Location 2 (outside the burn room). We also include the values from Location 3 to assess the extent to which the fire plume chemistry has been quenched.



DOI: 10.1002/fam

Table XIV. Yields of combustion products calculated from location 2 data.

| Gas | Fire stage | Sofa | Bookcase | Cable |
|---|---|---|---|---|
| $CO_2$ | Pre-flashover | $1.59 \pm 25\%$ | $0.50 \pm 50\%$ | $0.120 \pm 45\%$ |
| | Post-flashover | $1.13 \pm 25\%$ | $1.89 \pm 75\%$ | $1.38 \pm 15\%$ |
| CO | Pre-flashover | $1.44 \times 10^{-2} \pm 35\%$ | $2.4 \times 10^{-2} \pm 55\%$ | $5.5 \times 10^{-3} \pm 50\%$ |
| | Post-flashover | $5.1 \times 10^{-2} \pm 25\%$ | $4.6 \times 10^{-2} \pm 30\%$ | $1.48 \times 10^{-1} \pm 15\%$ |
| HCN | Pre-flashover | $3.5 \times 10^{-3} \pm 50\%$ | $4.6 \times 10^{-4} \pm 10\%$ | $6.3 \times 10^{-4} \pm 50\%$ |
| | Post-flashover | $1.5 \times 10^{-2} \pm 25\%$ | $2.5 \times 10^{-3} \pm 45\%$ | $4.0 \times 10^{-3} \pm 30\%$ |
| HCl | Pre-flashover | $1.8 \times 10^{-2} \pm 30\%$ | $2.2 \times 10^{-3} \pm 75\%$ | $6.6 \times 10^{-3} \pm 35\%$ |
| | Post-flashover | $6.0 \times 10^{-3} \pm 35\%$ | $2.2 \times 10^{-3} \pm 65\%$ | $2.1 \times 10^{-1} \pm 15\%$ |
| $NO_2$ | Pre-flashover | $<7 \times 10^{-2}$ | $<2 \times 10^{-2}$ | $<4 \times 10^{-3}$ |
| | Post-flashover | $<1 \times 10^{-3}$ | $<1 \times 10^{-3}$ | $<1 \times 10^{-3}$ |
| Acrolein | Pre-flashover | $<8 \times 10^{-3}$ | $<2 \times 10^{-3}$ | $<4 \times 10^{-4}$ |
| | Post-flashover | $<1 \times 10^{-4}$ | $<1 \times 10^{-4}$ | $<1 \times 10^{-4}$ |
| Formaldehyde | Pre-flashover | $<2 \times 10^{-2}$ | $<2 \times 10^{-3}$ | $<8 \times 10^{-4}$ |
| | Post-flashover | $<8 \times 10^{-4}$ | $<4 \times 10^{-4}$ | $<7 \times 10^{-4}$ |

Table XV. Fraction of combustible carbon appearing in carbon monoxide (NDIR, post-flashover data).

| Test | Location 1 | Location 2 | Location 3 |
|---|---|---|---|
| SW10 to SW14 | $0.031 \pm 0.008$ | $0.072 \pm 0.006$ | $0.068 \pm 0.007$ |
| BW3, BW4, BW6 | $0.071 \pm 0.007$ | $0.090 \pm 0.003$ | $0.069 \pm 0.026$ |
| BP1, BP2 | 0.080, 0.125 | 0.068, 0.100 | 0.060, 0.102 |
| PQ1, PQ2 | 0.073, 0.084 | 0.143, 0.152 | — |
| PW1, PW2 | 0.101 | 0.151, 0.151 | 0.147, 0.147 |

## 5. DISCUSSION

### *5.1. Overall test quality*

The most important outcome of this series of tests is a reliable, well-documented set of combustion product yields. This includes the numerical values themselves, the specific combustion conditions under which they were obtained, the uncertainty in their calculated values, and the repeatability of the tests.

Next most important is the initiation of the development of a standard protocol for obtaining yield values from a wider variety of test specimens. This includes test conduct procedures, experimental design, instrumentation, species sampling, and data reduction.

Third, it is important to evaluate the quality of the derived knowledge in the context of its intended use. The yield information would be used with a fire model (zone or CFD) to generate the time-dependent environment generated by a fire. Equations such as those in ISO 13571 [4] would then be used to assess whether the combination of occupancy design, contained combustibles, and occupant/responder characteristics lead to the desired level of life safety.

The documentation has been provided in the earlier sections of this paper. The following examines the context and quality of the results.



DOI: 10.1002/fam

### *5.2. Test repeatability*

Even under controlled laboratory conditions, attaining a reasonable degree of consistency in replicate fire tests requires both conceptual understanding of the phenomena and attention to detail. Even then, much of the success is attributed to art as well as science and engineering. In the current series, two to five tests of each of the complex fuels led to an appraisal of how likely the results from a single test might be representative. The results were within the range needed for the intended application.

The repeatability of the sofa tests was excellent: qualitative agreement of the shapes of the mass burning rate curves, similar global equivalence ratios, and low variability in the post-flashover yields. The repeatability of the $CO_2$, CO, and HCN yields was within $\pm 25\%$ and was within $\pm 35\%$ for HCl. The pre-flashover yield values were repeatable to within a factor of two. For the sofa tests that did not reach flashover, the mass burning rate curves were also similar and the later pre-flashover $CO_2$, CO, and HCl yields were repeatable to within $\pm 36\%$, with the HCN yields repeatable to within $\pm 45\%$. The yields from the two closed room sofa tests were repeatable to within $\pm 20\%$.

The results of the four cable tests (PQ1, PQ2, PW1, and PW2) indicated qualitatively similar results. Post-flashover yield repeatability was typically $\pm 15\%$ to 30%, with the pre-flashover repeatability somewhat higher, but within a factor of two.

For the four bookcase tests (BW3, BW4, BW6, and BW7) in which NDIR data were obtained, the repeatability was not as good as for the other combustibles. The post-flashover and pre-flashover yield repeatability values for $CO_2$ are ca. $\pm 75\%$ and $\pm 30\%$, respectively; the CO values are ca. $\pm 30\%$ and $\pm 55\%$. For the two bookcase tests for which we obtained FTIR data, the HCN post-flashover and pre-flashover yield repeatability values were ca. $\pm 45\%$ and 10%, respectively, and the HCl values were 65 and 75%. The post-flashover HCl yields from the three PVC sheet tests spanned over an order of magnitude.

The repeatability of the yield values obtained here for three of the combustibles is sufficient for the determination of whether a bench-scale apparatus is producing results that are similar to or different from the real-scale results here. The PVC sheet, from which only HCl yield data could be obtained, can only provide an indicator of appropriateness and then only for post-flashover simulation.

The repeatability results indicate an uncertainty in the fractional effective dose (FED) calculations in ISO 13571 that is comparable to the uncertainty in the equations themselves. This is especially so since a large fraction of fire deaths result from post-flashover fires (reducing the importance of the larger variance in the pre-flashover gas yields) and since CO is always a major incapacitating toxicant (reducing the importance of the variance in the other toxicants).

### *5.3. Species sampling and measurement*

*5.3.1. $CO_2$ and CO.* The $CO_2$ and CO yield data showed low variability and good consistency during the post-flashover period (Table VI). This was due in part to the fact that the upper layer, from which the gases were sampled, was well established and stable throughout a test. The $CO_2$ concentrations were high (ca. 5–10% by volume) and significantly above the sensitivity limit of the analyzers, and the sampling was reliably from the well-established upper layer. The scatter among replicate tests was about 20%, the lowest for any set of concentration measurements and not far from the estimated repeatability of the mass burning rate. The CO concentrations were



DOI: 10.1002/fam

also high (0.5–1% by volume) and showed repeatability similar to the $CO_2$ results. As indicated in Section 4.3, the FTIR and NDIR instruments showed good agreement for both gases.

The same was true at Location 2 during the late pre-flashover period in tests SW1 through SW3 (Table XIII), despite some of the concentrations being approximately an order of magnitude lower than after flashover. However, during the *general* pre-flashover burning periods for all tests, including the earlier pre-flashover periods in tests SW1 through SW3, distinctly higher variability was observed. Concentrations were yet another order of magnitude lower. Care was needed to adjust the sampling time period such that the thermocline showed the probe tip was sampling from the upper layer. Turbulence in the effluent stream was likely to result in non-uniform mixing with lower layer air. The burning rates of replicate tests varied more during the early growth period than later on.

Each cell in Table VII represents the volume fraction or yield integrated from the beginning of the test to that point in time. The values are probably somewhat high, since the sampling was performed at only one point near the top of the upper layer, and it was likely that there was a decreasing concentration gradient from the ceiling downward. The early NDIR yields for $CO_2$ and CO were remarkably close to those for the open door sofa tests (Tables VI and XIV). As the fire progressed, the $CO_2$ yield decreased and the CO yield increased, as expected from burning in an increasingly vitiated atmosphere.

*5.3.2. HCl and HCN.* The concentrations of these gases were only measured using FTIR. Thus, the same sampling considerations that were discussed above apply here. To mitigate errors in the calculated yields, we used the ratios of the concentrations and yields of HCl and HCN to the corresponding values for $CO_2$, as described above.

The HCl concentration data from the PVC sheet tests were high enough to obtain post-flashover HCl yields. Section 4.5 and Table XI show that the yield values from the multiple tests have a high degree of scatter and that the yields are at least as high as the notional yield. These findings most likely result from the HCl being pyrolyzed from the test specimen faster than the carbon-containing species. It is not likely that this is due to an artifact of the HCl measurement for two reasons. First, the FTIR instruments were carefully calibrated. Second, if the FTIR spectra were indicating high yield values, the CO and $CO_2$ yield results should also be high. Table VIII indicates only modest deviations from unity in the yields of CO and $CO_2$ between the two types of instruments.

The post-flashover Location 4 measurements for HCl and HCN were high enough to obtain estimates of the degree of loss of the compounds down the length of the corridor. By contrast, nearly all the pre-flashover showed a high degree of uncertainty and are not useful for even a rough estimate of losses down the corridor.

The two closed-room sofa tests, SC1 and SC2, produced very repeatable yield results for these two gases, the exception being a burst of HCl early in SC2.

*5.3.3. Other gases.* The equations in ISO 13571 include additional gases to be included in estimating the time available for escape or refuge from a fire: HBr, HF, $SO_2$, $NO_2$, acrolein ($C_3H_4O$), and formaldehyde ($H_2CO$). There was no Br, F, or S in any of the products examined in this project, so the first three of these gases were not expected. The presence of the latter three was not detected, thus establishing the upper limits of their presence at $100 \times 10^{-6}$, $10 \times 10^{-6}$, and $50 \times 10^{-}6$ volume fraction, respectively.

All three of these gases are sensory irritants. Their incapacitation concentrations from ISO 13571, their ratios normalized to HCl, and the concentration (Location 2, post-flashover) ratios of



DOI: 10.1002/fam

Table XVI. Limits of importance of undetected toxicants.

| | Volume fraction $\times 10^6$ | | | | Ratio to [HCl] | | | |
|---|---|---|---|---|---|---|---|---|
| | HCl | $NO_2$ | $C_3H_4O$ | $H_2CO$ | HCl | $NO_2$ | $C_3H_4O$ | $H_2CO$ |
| Incapacitating level | 1000 | 250 | 30 | 250 | 1.00 | 0.25 | 0.030 | 0.25 |
| Sofa | 800 | <100 | <10 | <50 | 1.00 | <0.12 | <0.012 | <0.06 |
| Bookcase | 20–200 | <100 | <10 | <50 | 1.00 | <5−0.5 | <0.5−0.05 | <2.5−0.25 |
| Cable | 1400 | <100 | <10 | <50 | 1.00 | <0.007 | <0.0007 | <0.04 |
| PVC sheet | 8000 | <100 | <10 | <50 | 1.00 | <0.012 | <0.0012 | <0.006 |

the gases in this study are shown in Table XVI. The measured pre-flashover concentrations were too low to obtain usable comparison.

From this analysis, the maximum concentrations of $NO_2$, formaldehyde, and acrolein that could have been present would have had secondary contributions to incapacitation relative to the concentrations of HCl in the sofa, cable, and PVC sheet tests. In the bookcase tests, where the HCl levels were low, the other irritants might be important. However, the high levels of CO in those tests suggest a secondary role for the irritant gases in causing incapacitation.

Levin *et al.* have developed extensive information on the effects of gas mixtures on rat lethality and incapacitation [25]. They used those data to test whether the toxic potency of a small number of gases could account for the lethality of the effluent from a variety of materials. The apparatus conditions were typical of pre-flashover combustion. Within the uncertainty in the results, ±30%, there was no need to invoke additional toxicants. Combined with the results obtained here for post-flashover conditions, it suggests that a set of upper limit yields for these gases would be a reasonable criterion for the accuracy of a bench-scale apparatus.

*5.3.4. Species measurement using FTIR spectroscopy.* There is considerable interest in adding FTIR spectroscopic analysis to fire test apparatus. A major European program [26] developed extensive information on the technique, and there are documents under development in ISO TC92 SC1 and ISO TC92 SC3 to standardize the implementation, such as ISO 19702 [27].

We were able to obtain usable information using this technique. There are a number of lessons emerging from this test series that can provide useful input to these efforts, such as the following:

- The application of FTIR spectroscopy to fire testing requires the constant attention of an experienced professional at a level well beyond the demands of the more traditional fire test instrumentation.
- To maximize the opportunity for obtaining time-dependent concentration data, we selected a small volume cell of short optical path length and operated without a soot filter. While some cleaning was necessary, it was not a major impediment. The short path length did limit the sensitivity, but did not seriously compromise our ability to determine toxicologically important levels of the major gases, as noted above.
- The long, heated lines used here (and recommended in the SAFIR report [26]) and the absence of filtration to remove the soot enabled quantitative collection of HCl, a compound that is generally regarded as difficult to determine.



DOI: 10.1002/fam

### 5.4. Loss of acid gases during transport

In light of the above discussion, we used only post-flashover data in the estimation of the degree to which HCl and HCN were lost to walls or deposited on smoke aerosol. In interpreting the data, one must recognize that the discussion often involves a small number of tests.

The first observation is that the NDIR data indicate about a factor of two dilution of the two fixed gases, CO and $CO_2$, with air from the lower layer for all combustibles (Table XIII). From there, the picture becomes more complex. The $CO_2$ data from the FTIR analyzers gave results that are similar to the NDIR data. However, the data for the other effluent components show distinct dependence on the combustible.

- The FTIR-measured CO concentration changes differed significantly from the NDIR-measured changes for the sofas and cable.
- The CO, HCl, and HCN concentrations generally decreased by similar factors for a given combustible, even though the factors were combustible-dependent. [The exception to this was HCN from the cable and bookcase/PVC fires, the reason for which is unknown.] The bookcase results were similar to the dilution of $CO_2$. The sofa, bookcase/PVC, and cable factors were more severe.

The cause of these variable effects is not understood. However, soot particles and aqueous aerosols are characterized by their number density, surface area, and hydrophilia. In these tests, only the soot *mass* was measured. It may well be that the smokes from the sofa, PVC, and cable materials have a greater affinity for acid gases and CO than does the smoke from the bookcases.

The inference we draw from these results is that for large fires of some combustibles, there can be little loss of reactive gases. This is consistent with a previously reported analysis of other experimental data [28]. However, for some other combustibles, loss factors of two to five beyond dilution are possible. Care should be taken not to generalize these limited findings to other commercial products without further study. In the absence of a comprehensive study of the relationship between smoke character and gas absorption, safety engineers are most likely to continue to assume there is no loss of toxicants, the more conservative approach.

### 5.5. Yield values

During vigorous post-flashover combustion, the yields of $CO_2$ and HCl should approach their notional values. As can be seen from Table X, the post-flashover values of $CO_2$ from all three combustibles do just that, given the conversion of up to ca. 10% of the carbon to carbonaceous smoke and CO and some formation of carbonaceous char residue. Under pre-flashover conditions, the $CO_2$ fraction from the sofas was as large as expected. However, for unknown reasons, the bookcase and cable fractions were far lower. In the closed room sofa tests, the yield began at about the notional level, then declined to about half that as room vitiation affected the completeness of combustion.

The HCl yields were close to notional under post-flashover conditions for the sofas, bookcases, and cable arrays. By contrast, in prior work [29], ca. 40% or less of the HCl from room-scale tests reached the analyzers. We attribute the present improvement to the use of calcium silicate walls (rather than drywall), the use of heated transfer lines to the FTIR spectrometers, and the absence of soot filters in those transfer lines. The somewhat lower value for the power cable may reflect the known HCl reaction with the calcium carbonate filler in the cable jacket.



DOI: 10.1002/fam

The pre-flashover stages of the sofa tests and the post-flashover stages of the PVC/bookcase tests produced HCl yields well above the notional values. The cause of these is unexplained. However, in both cases, relatively little of the specimen mass was volatilized, and it is possible that a disproportionate fraction of the effluent was decomposed fire retardant (sofa tests) or HCl (PVC tests).

Generally little of the nitrogen in the combustibles ends up in HCN. The observed exceptions were with the urea formaldehyde resin in the bookcase particle board and the nylon in the wire insulation, where over 10% of the N atoms appeared in HCN. This is consistent with the results of prior room-scale tests with a different urethane foam [29] in which 5–10% of the fuel nitrogen appeared in HCN and where (as noted above) the sampling of reactive gases was less efficient.

It is interesting to note that the addition of the PVC sheet to the bookcase fires led to an order of magnitude increase in the yield of HCN (Table VI). Perhaps, the flame inhibition by the chlorine atoms reduced the ability of the flame radicals to oxidize the HCN to one of the nitrogen oxides. Otherwise, Table X shows only modest differences in the conversion of fuel nitrogen to HCN despite large differences in the chlorine content of the fuel.

The early NDIR yields in the closed-room tests (Table VII) are consistent with the pre-flashover yields from the equivalent (late pre-flashover) phase of open room tests SW1 through SW3 (Table VI). [Note that the first entries in Table VII occur at 150 s; prior to that, the mass loss and concentration values were too small and noisy to obtain reliable ratios.] As noted above, the FTIR-derived CO and $CO_2$ yields are consistently somewhat lower than their NDIR-derived counterparts. However, the ratios of the yields of HCN and HCl to the FTIR-derived $CO_2$ yield are a fair basis for comparison and are similar to the later pre-flashover phase of tests SW1 through SW3. Because the mass burning rate fell sharply as the oxygen concentration dropped, the yields from SW1 through SW3 can be used to approximate the overall yields from the closed room tests. The volume fraction section of Table VII does not show evidence of large increases in the rates of generation or the yields of HCN or CO as the fires approached extinction.

Of most interest are the post-flashover yields of CO. A number of room-scale fire studies have indicated that the yield of CO is approximately 0.2 (g CO/g fuel consumed) and that this value is not very dependent on the combustible [30]. [Much higher yields have been observed when significant quantities of wood products are present in the upper layer of the fire room [31]]. In the current study, the NDIR-derived post-flashover CO yields from the cable fires approach this value, with a mean value of ca. 0.15 g/g. The sofas and bookcases appear to generate about one-fourth of the expected value (Table VI).

A first consideration is whether the tests truly reached flashover. Examination of the test videos and data logs indicate that each 'declaration of flashover' occurred when key characteristics were observed: significant oxygen depletion within the fire room, high temperature in the upper layer of the burn room and in the upper portion of the doorway, flames out the doorway.

Experimental errors of a sufficient magnitude are highly unlikely. Since two different types of analyzers with independent sampling lines produced comparable CO yields, the difference from the expected value cannot be attributed to an instrumental or sampling error. Since the same calculations produced $CO_2$ yields near the notional limits, there cannot be a missing factor in the data reduction.

It is possible that a large amount of CO was formed in the room, but was oxidized in the secondary burning at the doorway. Computer simulations of room fires using FDS indicate that the environment at Location 1 should have been highly vitiated and that the CO should have been



DOI: 10.1002/fam

at its peak there. The test records indicate low oxygen levels. However, Table XV shows that the fraction of fuel carbon appearing in CO is actually lower at Location 1 than at Location 2.

A more likely hypothesis is as follows. A large quantity of pyrolyzate was generated post-flashover. Much of this consumed the limited available oxygen, forming CO, but leaving much of the organic matter unoxidized. As these gases reached the doorway and began to entrain fresh air, more of the organic matter was oxidized to CO. Some of the CO was also oxidized to $CO_2$. Combined, these processes set up a dynamic situation where the observed $[CO]/[CO_2]$ ratio and the yield of CO depended on the degree of air-effluent mixing and the rate of cooling of the total flow. However, this is speculative; and, at present, there is no firm explanation for this behavior.

Different fires and different stages of those fires are likely to be accompanied by differing degrees of CO formation and burnout. Thus, we suggest that for fire hazard and risk assessments, one should use the CO yield value of 0.2 g CO per g fuel consumed. Bench-scale combustors typically used for generating toxic potency data generally do not have the potential for the secondary combustion processes described above. Thus, for assessing the accuracy of the data from such apparatus, it is also appropriate to use the CO yield value of 0.2 g CO per g fuel consumed.

### *5.6. Use of the results*

The yield data developed here are ready for use in determining whether and how to use a bench-scale apparatus for generating toxic potency data of known accuracy. Generically, the following steps are suggested:

- Combust samples of these specimens in the bench-scale device under a range of combustion conditions appropriate for well-ventilated and underventilated fires.
- Determine the degree to which agreement is reached with the yields measured here.
- For the gases whose yields here were below the detection limits, determine whether the bench-scale results are consistent with these detection limits.
- For the post-flashover yield of CO, use the CO yield value of 0.2 g CO per g fuel consumed, keeping in mind that some room-scale studies (especially with wood products in the upper layer) have measured post-flashover yields significantly larger than the values determined here.
- Appropriate weighting of the comparisons for individual gases can be derived using the equations in ISO 13571.

## 6. CONCLUSION

It is important to be able to demonstrate how well a bench-scale toxic potency measurement apparatus reflects the effluent produced in real fires of the same combustible. This report documents the measurement of the yields of the prime toxicants ($CO_2$, CO, HCl, HCN) and smoke from the combustion of three complex products (sofa cushions, bookcases, and power cable) in a room connected to a long corridor. There are results for both the pre-flashover and post-flashover stages of the fires, with additional post-flashover yield data on a PVC material.

The repeatability of the yield values obtained here is sufficient for the determination of whether a bench-scale apparatus is producing results that are similar to or different from the real-scale results here.



DOI: 10.1002/fam

The uncertainty in the post-flashover data is smaller due to the larger species concentrations and the more fully established upper layer from which the fire effluent was sampled. The toxicant yields from sofa cushion fires in a closed room were similar to those from pre-flashover fires of the same cushions in a room with the door open.

Since a large fraction of United States fire deaths result from post-flashover fires [32], and since CO is always a major (if not the dominant) incapacitating toxicant, the repeatability results indicate an uncertainty in the FED calculations that is comparable to the uncertainty in the equations themselves.

Other toxicants ($NO_2$, formaldehyde, and acrolein) were not found. Concentrations below the detection limits were shown to be of limited toxicological importance relative to the detected toxicants.

The use of FTIR spectroscopy was shown to be a useful tool for obtaining toxicant concentration data. However, its operation and interpretation are far from routine. The agreement between the FTIR instruments and conventional non-dispersive infrared analyzers was not consistently good, but was reasonable enough to identify situations where the effluent sampling may have been compromised and where signals were approaching the background limits.

Measurements at both ends of the corridor provided an indication of the degree to which the combustion product concentrations decreased relative to simple dilution. The losses of CO, HCN, and HCl were found to be dependent on the combustible. The downstream to upstream concentration ratios varied from unity for some fuels to a factor of five smaller for others.

The yield of CO for the sofa and bookcase tests was significantly lower than the expected value of 0.2, while the CO yield for the cable tests was close. The determinations were shown to be accurate. It is suggested that one should use the CO yield value of 0.2 g CO per g fuel consumed for both fire safety analyses and for assessing the accuracy of bench-scale combustors for generating toxic potency data.

## ACKNOWLEDGEMENTS

The authors express their appreciation for the contributions of many people in bringing success to such an expansive project. George Mulholland designed the smoke sampling apparatus, which was built and operated by Michael Selepak; Dr. Mulholland and Jenny Oran analyzed the data. David Stroup operated the large-scale test facility and with Lauren DeLauter and Gary Roadarmel built the room/corridor assembly and assisted in the tests. Jack Lee (R.I.P.) assisted in numerous ways during the room construction and test conduct. Jonathan Demarest also assisted with the tests and in reducing the data. Dr. Kurt Reimann of BASF provided information helpful in the design of the sofas; Douglas Wetzig of PolyOne supplied the PVC sheet; David Mercier of Southwire, Inc. provided useful information on the formulation of the cable. Schwartzkopf Laboratories performed the elemental and thermal analyses of the combustibles.

This research was sponsored by the National Institute of Standards and Technology, the Alliance for the Polyurethane Industry, the American Plastics Council, DuPont, Lamson & Sessions, Underwriters Laboratories, and the Vinyl Institute under the aegis of the Fire Protection Research Foundation and the supervision of Frederick Mulhaupt and Steven Hanly.

## REFERENCES

1. Phillips WGB, Beller DK, Fahy RF. Computer Simulation for fire protection engineering, Chapters 5–9. In *SFPE Handbook of Fire Protection Engineering* (3rd edn), DiNenno PJ (ed.). NFPA International: Quincy, MA, 2002.
2. FDS. *Fire Dynamics Simulator*, downloadable from http://www.fire.nist.gov/fds.
3. CFAST. *Consolidate Model of Fire and Smoke Transport*, downloadable from http://cfast.nist.gov.



DOI: 10.1002/fam

4. ISO 13571. *Life-threatening Components of Fire–Guidelines for the Estimation of Time Available for Escape Using Fire Data*, International Standards Organization, Geneva, 2007.
5. Neviaser JL, Gann RG. Evaluation of toxic potency values for smoke from products and materials. *Fire Technology* 2004; **40**:177–200.
6. Kaplan HL, Hartzell GE. Modeling of toxicological effects of fire gases: I. Incapacitating effects of narcotic fire gases. *Journal of Fire Sciences* 1984; **2**:286–305.
7. Kaplan HL, Grand AF, Hartzell GE. *Combustion Toxicology*: *Principles and Test Methods*. Technomic Publishing Co, Inc.: Lancaster, PA, 1983.
8. ISO 19706. *Guidelines for Assessing the Fire Threat to People*, International Standards Organization, Geneva, 2007.
9. ISO 16312–1. *Guidance for Assessing the Validity of Physical Fire Models for Obtaining Fire Effluent Toxicity Data for Fire Hazard and Risk Assessment—Part 1*: *Criteria*, International Standards Organization, Geneva, 2006.
10. ISO/TR 16312–2. *Guidance for Assessing the Validity of Physical Fire Models for Obtaining Fire Effluent Toxicity Data for Fire Hazard and Risk Assessment—Part 2*: *Evaluation of Individual Physical Fire Models*, International Standards Organization, Geneva, 2007.
11. Gann RG, Averill JD, Nyden MR, Johnsson EL, Peacock RD. *Smoke Component Yields from Room-Scale Fire Tests*, *NIST Technical Note 1453*, National Institute of Standards and Technology, Gaithersburg, MD, 2003.
12. Pitts WM, Braun E, Peacock RD, Mitler HE, Johnsson EL, Reneke PA, Blevins LG. Temperature uncertainties for bare-bead and aspirated thermocouple measurements in fire environments, U.S./Japan Government Cooperative Program on Natural Resources, Fire Research and Safety, *Proceedings of the 14th Joint Panel Meeting*, Tsukuba, Japan, 1998; 240–247.
13. Newman JS, Croce PA. A simple aspirated thermocouple for use in fires. *Journal of Fire and Flammability* 1979; **10**:326–336.
14. Peacock RD, Bukowski RW, Reneke PA, Averill JD, Markos SH. Development of a fire hazard assessment method to evaluate the fire safety of passenger trains. *Proceedings of the Fire and Materials 2001 Conference*, Interscience Communications, London, 2001; 67–78.
15. Heskestad G. In *Bidirectional Flow Tube for Fire-Induced Vent Flows in Large-Scale Bedroom Fire Test*, Croce PA, Emmons HW (eds). FMRC Serial 21011.4, Factory Mutual Research Corp.: Norwood, MA, 1974; 140–145.
16. Emmons HW. Vent Flows Chapter 2–3. In *SFPE Handbook of Fire Protection Engineering*, DiNenno PJ *et al*. (eds). NFPA International: Quincy, MA, 2002.
17. Haaland DM, Easterling RG, Vopicka DA. *Applied Spectroscopy* 1985; **39**:73–84.
18. *Gas Phase Infrared Spectral Standards*, *Revision B*, Midac Corp.: Irvine, CA, 1999.
19. Speitel LC. *DOT/FAA/AR-01/88*, Federal Aviation Administration, Atlantic City, 2001; 1–18.
20. Autoquant Users Guide. Midac Corp.; Irvine CA, 10–15 (1995–1999). See also the internal memo entitled 'Description of Classical Least Squares Analysis Technique and a Comparison of Two Correction Schemes for Non-Linearity in Measured Sample and Reference Absorbances', written by Plummer G, 2001.
21. Ohlemiller TJ, Villa K. *Furniture Flammability*: *An Investigation of the California Bulletin 133 Test. Part II Characterization of the Ignition Source and a Comparable Gas Burner*, *NISTIR 4348*, National Institute of Standards and Technology, Gaithersburg, MD, 1990.
22. Dey MK. *Evaluation of Fire Models for Nuclear Power Plant Applications Cable Tray Fires—International Panel Report*, *NISTIR 6872*, National Institute of Standards and Technology, Gaithersburg, MD, 2002.
23. Peacock RD, Davis S, Lee BT. *An Experimental Data Set for the Accuracy of Room Fire Models*, *NBSIR 88-3752*, National Bureau of Standards, Gaithersburg, MD, 1988.
24. Leonard S, Mulholland GW, Puri R, Santoro RJ. Generation of CO and smoke during underventilated combustion. *Combustion and Flame* 1994; **98**:20–34.
25. Levin BC, Braun E, Navarro M, Paabo M. Further development of the N-gas mathematical model: an approach for predicting the toxic potency of complex combustion mixtures. In *Fire and Polymers II*: *Materials and Tests for Hazard Prevention*, ACS Symposium Series 599, Nelson GL (ed.). American Chemical Society: Washington, DC, 1995; 293–311.
26. *Smoke Gas Analysis by Fourier Transform Infrared Spectroscopy*: *The SAFIR Project*, VTT Research Note, Technical Research Centre of Finland, 1999.
27. ISO 19702. *Toxicity Testing of Fire Effluents—Guidance for Analysis of Gases and Vapours in Fire Effluents Using FTIR Gas Analysis*, International Standards Organization, Geneva, 2007.
28. Gann RG, Averill JD, Butler K, Jones WW, Mulholland GW, Neviaser JL, Ohlemiller TJ, Peacock RD, Reneke PA, Hall Jr JR. *International Study of the Sublethal Effects of Fire Smoke on Survivability and Health SEFS Phase I*



DOI: 10.1002/fam

*Final Report* (*NIST*): *Technical Note 1439*, National Institute of Standards and Technology, Gaithersburg, MD, 2001.
29. Babrauskas V, Harris Jr RH, Braun E, Levin BC, Paabo M, Gann RG. *The Role of Bench-Scale Test Data in Assessing Real-Scale Fire Toxicity*, *NIST Tech Note 1284*, National Institute of Standards and Technology, Gaithersburg, MD, 1991.
30. ASTM E 1678–09. *Standard Test Method for Measuring Smoke Toxicity for Use in Fire Hazard Analysis*, ASTM International, West Conshohocken, PA, 2009.
31. Pitts WM. *The Global Equivalence Ratio Concept and the Prediction of Carbon Monoxide Formation in Enclosure Fires*, *NIST Monograph 179*, National Institute of Standards and Technology, Gaithersburg, MD, 1994.
32. Gann RG, Babrauskas V, Peacock RD, Hall Jr JR. Fire conditions for smoke toxicity measurement. *Fire and Materials* 1994; **18**:193–199.



DOI: 10.1002/fam